

Thermodynamic and Transport Properties of Polyhedral Oligomeric Silsesquioxanes in Poly(dimethylsiloxane)

Alberto Striolo,* Clare McCabe, and Peter T. Cummings

Department of Chemical Engineering, Vanderbilt University, Nashville, Tennessee 37235

Received: October 9, 2004; In Final Form: April 27, 2005

Polyhedral oligomeric silsesquioxane (POSS) molecules when functionalized appropriately and dispersed in polymers show promise as monodisperse organic–inorganic hybrid nanocomposite materials characterized by superior mechanical properties. We report here molecular-simulation results for POSS–POSS radial distribution functions, potentials of mean force, and self-diffusion coefficients for POSS monomers dissolved in poly(dimethylsiloxane) in the temperature range of 300–1000 K. Our results demonstrate that it is possible to modulate the effective POSS–POSS interaction by increasing the temperature or by substituting the hydrogen atoms in the POSS monomer with methyl groups. In addition, our results indicate that the motion of POSS monomers dissolved in poly(dimethylsiloxane) follows a hopping mechanism.

Introduction

The mechanical properties of traditional materials can potentially be improved through the incorporation of nanoscale particulates, yielding a nanocomposite material. Several types of nanocomposites and different fabrication routes have been proposed. For example, mixtures of polymers and clays^{1,2} and of polymers and silica³ prove to be effective even though the molecular structural units are polydisperse in both size and shape. In an effort to improve the material microstructure and to control its texture, carbon fibers have been covalently bound to polymer molecules,⁴ along with other precisely defined molecular entities.^{5–7} In this area, significant interest is currently being devoted to nanocomposites based on polyhedral oligomeric silsesquioxanes (POSS), which are cages of silicon and oxygen having the formula $(\text{SiO}_{1.5})_8\text{R}_8$, where R is an organic group.⁸ In Figure 1, we present a schematic representation of the simplest POSS monomer in which R is a hydrogen atom, $(\text{SiO}_{1.5})_8\text{H}_8$. Because POSS chemistry is extremely flexible, a wide variety of organic substituents, including alcohols, chlorosilanes, epoxides, esters, isocyanates, acrylates, silanes, etc.,⁹ have been substituted for one or all of the hydrogen atoms in the POSS cage. Clearly, different functional groups will impart different physical properties (e.g., solubility of the monomer in common solvents^{10,11}), suggesting a wide range of potential applications for POSS-based nanocomposites. For example, because of their chemical flexibility, POSS monomers are suitable for modifying interfacial properties,^{12–15} they are promising catalysts,^{16,17} and they can be used as nanoscale building blocks^{18,19} and to form water-soluble hybrid micelles^{20–22} and nanocomposite foams^{23,24} and to synthesize hyperbranched or cross-linked polymers.^{25–27}

POSS monomers have been incorporated as fillers in several polymers, including siloxanes, styryls, and poly(propylene).²⁸ When POSS monomers are used as fillers in poly(propylene), they affect the crystallization rate of the material. It is believed that at low concentrations POSS monomers provide crystallization nuclei for quiescent crystallization, but at higher

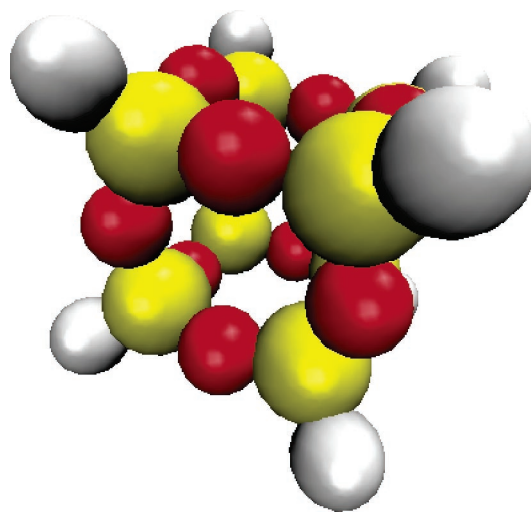


Figure 1. Schematic representation of a POSS monomer. Yellow, red, and white spheres represent silicon, oxygen, and hydrogen atoms, respectively. In the octa-functionalized POSS monomer considered here, the hydrogen atoms are substituted with methyl groups.

concentrations, their distribution in the material prevents the molecular motion of the polymer chains, thus reducing the crystallization rate.²⁸ When POSS monomers used as fillers phase separate, the properties of the resulting material are, at best, similar to those of the parental polymer.²⁹ To achieve enhancement of the mechanical properties in these POSS–polymer systems, it is convenient to chemically bind small amounts of POSS monomers to the polymer chains to promote uniform dispersions in the material. Materials obtained in this manner include copolymers of polysiloxane,^{15,30} poly(methyl methacrylate),^{31,32} poly(4-methylstyrene),³³ poly(norbornyl),³⁴ polyurethane,³⁵ poly(acetoxystyrene) and poly(vinylpyrrolidone),³⁶ polyethylene,^{37,38} and poly(propylene).³⁸ Enhanced properties of POSS-based hybrid copolymers include increased thermal stability, higher glass transition temperatures, increased flame and heat resistance, and enhancement in the modulus and melt strengths.^{39,40}

Despite this large body of experimental work on POSS–polymer systems, neither the microstructure of the copolymers

* To whom correspondence should be addressed. E-mail: Alberto.Striolo@Vanderbilt.edu

TABLE 1: Potential Parameters for the Molecular Models Employed in This Work

bond	r_0 (Å)	k_b (kcal mol ⁻¹ Å ⁻²)	
Si-O	1.64	350.12	
Si-CH ₃	1.90	189.65	
angle	θ_0 (deg)	k_θ (kcal mol ⁻¹ rad ⁻²)	
Si-O-Si	146.46	14.14	
O-Si-O	107.82	94.50	
CH ₃ -Si-CH ₃	109.24	49.97	
O-Si-CH ₃	110.69	49.97	
dihedral	c_1 (kcal/mol)	c_2 (kcal/mol)	c_3 (kcal/mol)
Si-O-Si-O	0.2250	0.0000	0.0000
Si-O-Si-CH ₃	0.0000	0.0000	0.0100
nonbonded interaction	σ_{ij} (Å)	ϵ_{ij} (kcal/mol)	
Si-Si	4.29	0.1310	
O-O	3.30	0.0800	
Si-O	3.94	0.0772	
CH ₃ -CH ₃	3.75	0.1947	
Si-CH ₃	3.83	0.1596	
O-CH ₃	3.38	0.1247	

nor the mechanism of reinforcement is well understood. The changes in thermodynamic and mechanical behavior can be attributed to factors such as the size of the POSS monomer, the nature of the organic periphery, the number of reactive functionalities, the concentration and solubility of POSS monomers in the material, etc. These and other factors determine whether POSS monomers are incorporated as isolated and uniformly dispersed molecules, isolated phase-separated particles, or matrix-bound aggregates.^{35,36,38} Understanding and controlling the aggregation and crystallization of polymers containing silsesquioxanes will enable us to design materials with tailored properties for selected applications.⁴¹ In this scenario, molecular simulation appears to be an ideal tool for understanding how the presence of POSS monomers may modify, and eventually enhance, the mechanical properties of polymeric materials. For example, through a combination of experimental and simulation studies, it has been shown that POSS monomers with flexible tethers reduce the glass transition temperature and elastic moduli of epoxi resins, but provide higher fracture toughness, while POSS monomers with rigid tethers provide higher glass transition temperatures and elastic moduli, but reduce the fracture toughness.⁴² In a different approach, molecular dynamics simulations for norbornene polymers with pendant POSS monomers⁴³ have suggested that POSS monomers enhance the thermal and elastic properties of the copolymers because they inhibit the motion of polymer chains.

In this work, we focus on the thermodynamic properties of POSS monomers dissolved in poly(dimethylsiloxane) (PDMS) with a molecular weight of 1200 g/mol. The aim of our work is to understand if the properties of the POSS-enriched material can be tailored by changing the organic moieties of the POSS cubes. We consider two representative POSS monomers: bare POSS, (SiO_{1.5})₈H₈, and octa-functionalized POSS in which the hydrogen atoms are substituted with methyl groups. We conduct atomistic molecular dynamic simulations in the temperature range of 300–1000 K. While the real materials may decompose at the highest temperatures considered here, our results may suggest experimental strategies for the synthesis of materials with prescribed structural properties. After presenting the simulation method, in the remainder of the paper we report

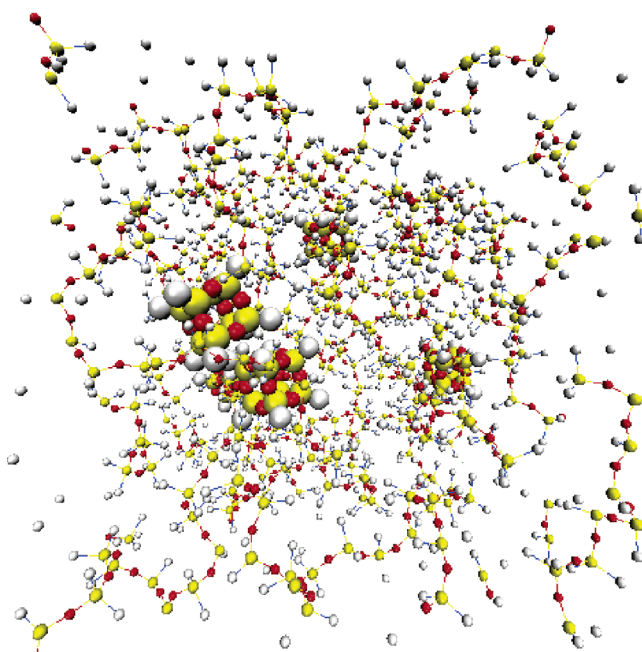


Figure 2. Schematic representation of a system composed of five octa-functionalized POSS monomers dissolved in PDMS at 600 K. Yellow, red, and white spheres represent silicon, oxygen, and methyl groups, respectively. POSS atoms are enlarged for visualization purposes.

results for the effective pair potential of mean force between POSS monomers and their diffusion coefficients when dissolved in poly(dimethylsiloxane) at 300, 400, 600, and 1000 K. Our results are the first reported data for both the effective pair potential of mean force between POSS monomers dissolved in other macromolecules and their diffusion coefficients. Although no experimental data (i.e., neutron scattering) are available to support our predictions, our results are useful for implementing coarse-grained simulations toward the design of novel materials,^{44,45} and for obtaining parameters for the theoretical prediction of phase equilibria.⁴⁶

Simulation Details

Force Fields. The PDMS molecules are described using a collapsed-atom force field that satisfactorily reproduces the radial distribution functions of liquid PDMS.⁴⁷ POSS monomers are described using the same model that was used for PDMS. The hydrogen atoms in the bare POSS monomer are not involved in dispersive interactions, but they are included in the calculation of short-range potentials that determine the structure of the POSS cage. The methyl groups, either in the POSS monomer or in the PDMS monomer, are treated in a united-atom approach according to the TraPPE force field.⁴⁸

In the force fields that were employed, atoms in the same molecule interact with each other via short-range potentials that account for bond length, bond angles, and torsional constraints. Bond-length fluctuations around the equilibrium separation r_0 are subject to a harmonic functional form:

$$V_b(r) = k_b(r - r_0)^2 \quad (1)$$

Similarly, bond-angle oscillations about the equilibrium angle θ_0 are subject to harmonic constraints:

$$V_a(\theta) = k_a(\theta - \theta_0)^2 \quad (2)$$

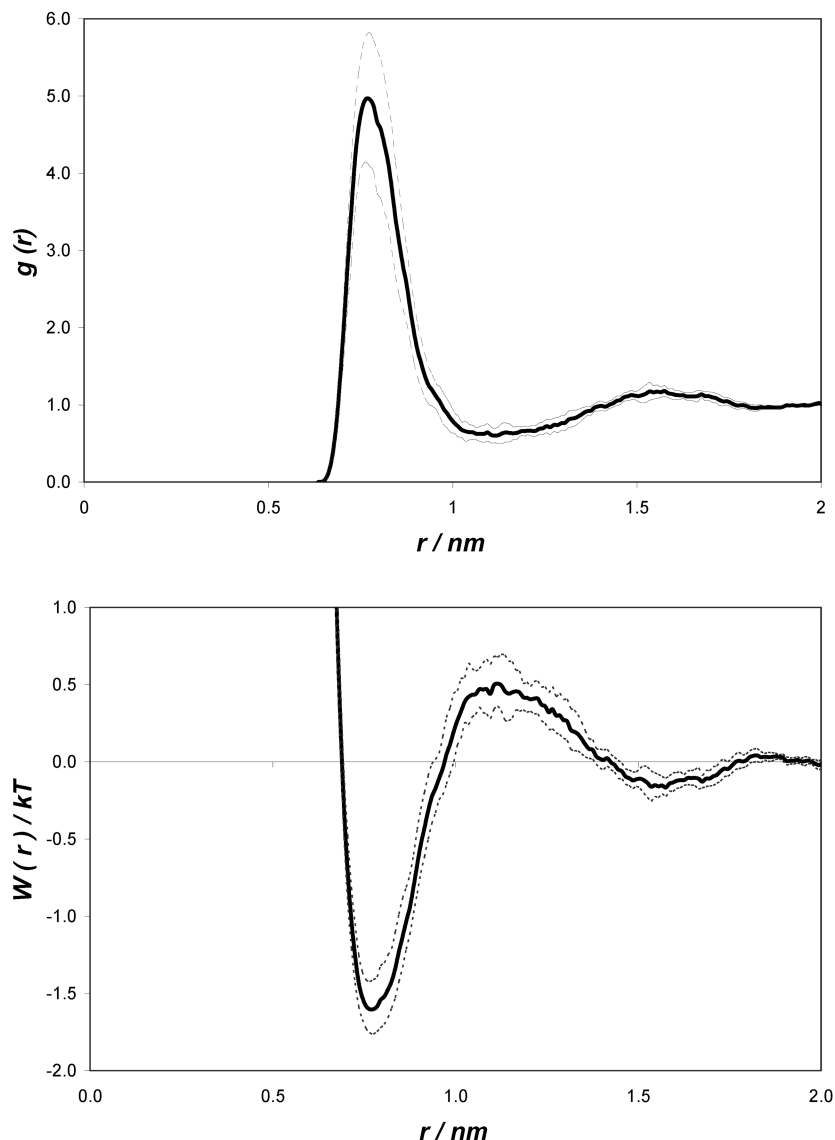


Figure 3. Radial distribution function (top) and effective pair potential of mean force (bottom) between bare POSS monomers dissolved in PDMS as a function of the center-to-center distance between centers of mass of the POSS monomers. Results are reported for 400 K (black solid line). The gray dotted lines delimit the statistical uncertainties (standard deviation) of the results reported here.

Torsional-angle fluctuations ϕ are subject to a torsional potential with the functional form:

$$V_t(\phi) = c_1[1 + \cos(\phi)] + c_2[1 - \cos(2\phi)] + c_3[1 + \cos(3\phi)] \quad (3)$$

In eqs 1–3, V_b , V_a , and V_t are the bond, angle, and torsional potentials, respectively, k_b , k_a , c_1 , c_2 , and c_3 are proportional constants, and r , θ , and ϕ are the instantaneous bond length, bond angle, and torsional angle, respectively.

In addition to intermolecular forces, Lennard-Jones 12-6 potentials describe nonbonded $\text{CH}_3\text{--CH}_3$, $\text{CH}_3\text{--O}$, and $\text{CH}_3\text{--Si}$ dispersive interactions:

$$u(r_{ij}) = 4\epsilon_{ij} \left[\left(\frac{\sigma_{ij}}{r_{ij}} \right)^{12} - \left(\frac{\sigma_{ij}}{r_{ij}} \right)^6 \right] \quad (4)$$

and Lennard-Jones 9-6 potentials describe non-bonded Si-O dispersive interactions:

$$u(r_{ij}) = \epsilon_{ij} \left[2 \left(\frac{\sigma_{ij}}{r_{ij}} \right)^9 - 3 \left(\frac{\sigma_{ij}}{r_{ij}} \right)^6 \right] \quad (5)$$

Parameters ϵ_{ij} and σ_{ij} have the usual meaning. r_{ij} is the distance between atoms i and j . Nonbonded interactions between atoms in the same molecule are not accounted for unless the pairs of atoms are separated by more than three bonds, consistent with many formalisms, including the TrAPPE force field.⁴⁸ In Table 1, we report the parameters used to implement the force fields described herein.

Simulation Algorithm. Classical molecular dynamics simulation techniques are employed to study the thermodynamic and transport properties of systems containing POSS monomers and PDMS with a molecular weight of 1200 g/mol. The systems considered are composed of five POSS monomers and 24 PDMS chains diluted in a 4.0 nm cubic simulation box. The total number of PDMS molecules is chosen to achieve a total density in the systems of approximately 0.8 g/cm³. A representative snapshot of one simulated system in which octa-functionalized silsesquioxane monomers are dissolved in PDMS at 600 K is shown in Figure 2.

To integrate the equations of motion, we use the DL-POLY simulation suite⁴⁹ in the canonical (NVT) ensemble.⁵⁰ The temperature is adjusted using the Nosé-Hoover thermostat. For selected systems, the thermostat time constant was varied among

the values of 0.5, 1.0, and 2.0 ps. No difference was observed in any of the quantities that were considered. The majority of the simulations are performed with a time constant of 1.0 ps. The integration time is 1 fs at ≤ 400 K and 0.5 fs at higher temperatures. The initial configurations are obtained using a Monte Carlo procedure developed for the study of colloid-polymer systems.⁵¹ The POSS monomers are placed in the simulation box with one molecule located in the box center and the other four along the box main diagonals. The PDMS chains are then built using periodic boundary conditions in all directions. At this stage, the building subroutine merely ensures that the connectivity between different polymer segments is respected and that different polymer segments do not overlap either with each other or with the POSS monomers. The complete interatomic potentials are switched on in all the subsequent simulation phases. These initial configurations are relaxed at elevated temperatures (1000 K) for 500 ps. Relaxed configurations are then brought abruptly to the temperatures of interest, and at each temperature, the first 500 ps of simulation data are discarded to allow for complete relaxation (i.e., the total energy reaches a plateau). The production phase lasts 4 ns at each temperature that is considered. One system configuration is stored every 500 fs. These configurations are then used to compute the radial distribution function between the centers of mass of the POSS monomers. From the radial distribution function, the effective potential of mean force between pairs of POSS monomers is computed according to⁵²

$$\frac{W(r)}{kT} = -\ln[g(r)] \quad (6)$$

where $W(r)$ and $g(r)$ are the potential of mean force and the radial distribution function at a separation r between the centers of mass of two POSS monomers, respectively, k is the Boltzmann constant, and T is the absolute temperature. The potential of mean force between two molecules at center-to-center separation r corresponds to the work done on the system to bring the two molecules from an infinite separation to the distance r .⁵² From the potential of mean force, it is possible to obtain the excess thermodynamic properties of a system (see, for example, ref 53). To ensure the reliability of the results, we repeat the simulations at least four times for each system and temperature considered. Additionally, we estimate the uncertainty of our calculations by computing the standard deviation.

To determine the diffusion coefficient D for the POSS monomers, we computed the mean-square displacement, ΔR^2 , of the centers of mass of the POSS monomers as a function of time and used the Einstein equation:

$$D = \frac{1}{6} \lim_{t \rightarrow \infty} \frac{\Delta R^2}{dt} \quad (7)$$

To construct the mean-square displacement, we consider 10 origins separated by 200 ps and we average over the results obtained for the five POSS monomers present in the system. In what follows, we report the average diffusion coefficients obtained in our simulations. For comparison, we also compute the self-diffusion coefficient for the PDMS molecules. To estimate this quantity, we compute the mean-square displacement of the center of mass of each PDMS molecule and apply eq 7.

Results and Discussion

Radial Distribution Function. In Figure 3, we report representative results for the radial distribution functions and

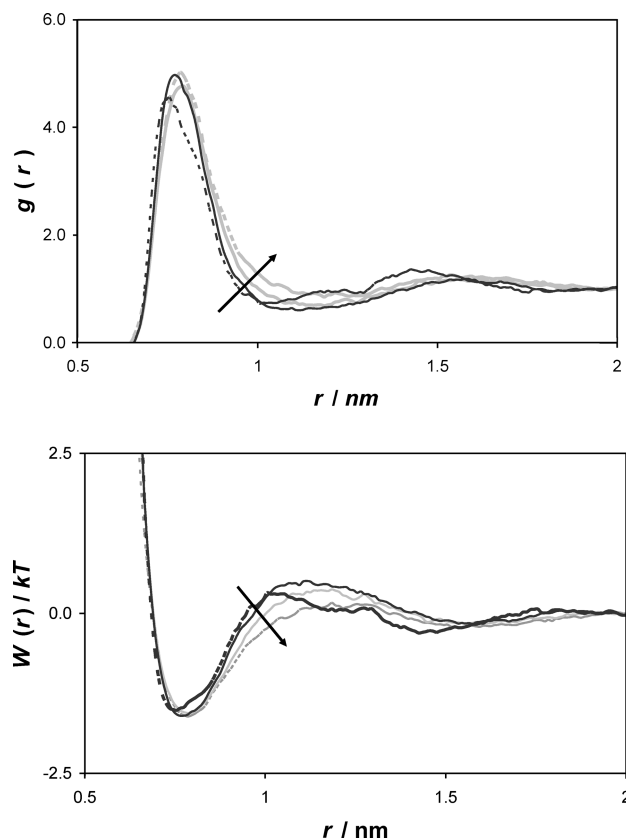


Figure 4. Radial distribution function (top) and effective pair potential of mean force (bottom) between bare POSS monomers dissolved in PDMS as a function of the center-to-center distance between centers of mass of the POSS monomers. Results are reported for several temperatures: black dotted lines for 300 K, black solid lines for 400 K, gray solid lines for 600 K, gray dotted lines for 1000 K. Statistical uncertainties are not reported for clarity. The arrows indicate results obtained as the temperature increases.

the potentials of mean force obtained for bare POSS monomers diluted in PDMS at 400 K. In this figure, we show the standard deviation for each computed quantity to establish the reliability of the results reported in this work. It should be noted that the results become more reliable as the temperature increases, but technological interest is greater for simulations conducted near room temperature, where the mobility of the macromolecules is reduced and the results are affected by larger uncertainties. The results reported in Figure 3 show that bare POSS monomers strongly attract each other. The first attractive peak in the radial distribution function, located at a center-to-center distance of approximately 0.78 nm, is followed by a midrange weak POSS-POSS effective repulsion, as observed when colloidal particles are in solution with short athermal polymers.^{51,54} The midrange repulsion is probably due to the packing of the PDMS molecules in the region between the two approaching POSS monomers when their separation is sufficient for one monomer to reside between the POSS monomers.⁵¹ The potential of mean force, obtained from the radial distribution function by using eq 6, reflects the characteristics just described in an effective POSS-POSS interaction potential. Bare POSS monomers attract each other at short separations; the peak of the attractive interaction is located at a center-to-center separation of approximately 0.78 nm, and the first attractive peak is followed by a midrange weak repulsion and by a longer-range modest attraction.

In Figure 4, we report the radial distribution function and the potential of mean force for bare POSS monomers dissolved in PDMS at 300, 400, 600, and 1000 K. The first peak of the

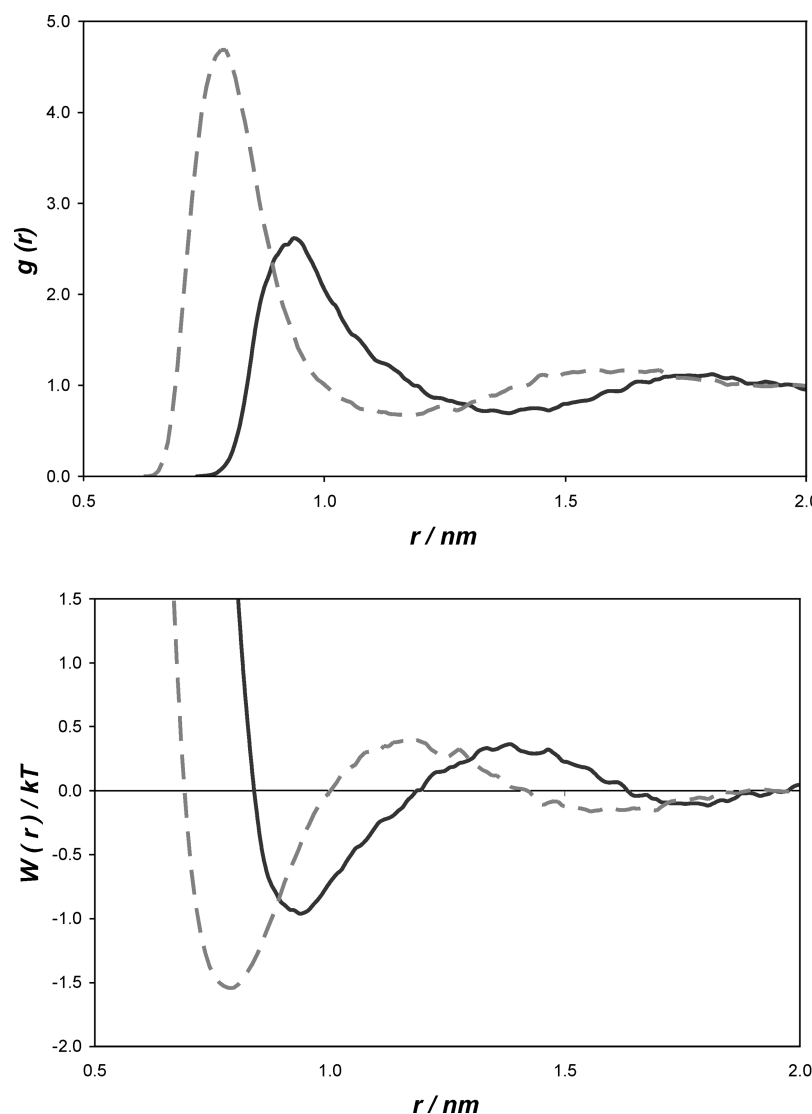


Figure 5. Radial distribution function (top) and effective pair potential of mean force (bottom) between POSS monomers dissolved in PDMS at 600 K. Gray broken lines depict data for bare POSS monomers while black solid lines data for octa-functionalized monomers. Statistical uncertainties are not reported for clarity.

radial distribution function is located at approximately 0.78 nm regardless of the temperature. As the temperature decreases, the midrange repulsion increases and the attractive peak becomes narrower. At large separations, the results obtained for both the radial distribution function and the potential of mean force do not show significant temperature effects.

It is instructive to investigate how the effective POSS–POSS interactions change when the hydrogen atoms in the bare POSS monomer are substituted with methyl groups. In Figure 5, we report the radial distribution function and the potential of mean force for bare and octa-functionalized POSS monomers in PDMS at 600 K. As expected, the attractive peak in the radial distribution function is shifted to larger center-to-center separations for octa-functionalized monomers (approximately 0.94 nm) because of the larger excluded volume due to the methyl groups. Also, at this temperature, the short-range attraction is significantly weaker for octa-functionalized than for bare POSS monomers. These results confirm that POSS–POSS interactions can be easily tailored by substitution of the hydrogen atoms with other chemical groups. In particular, it should be noted that the octa-functionalized POSS monomers considered here are chemically similar to PDMS, whereas the bare POSS monomers are not. Because they are chemically more compat-

ible, we expect a weaker effective attraction between octa-functionalized monomers dissolved in PDMS than for bare POSS dissolved in PDMS. This scenario, however, is not observed at low temperatures (300 or 400 K; comparative results not shown for brevity) where the attractive peak of the radial distribution function is similar in intensity when either bare or octa-functionalized POSS monomers are dissolved in PDMS.

In Figure 6, we report results for the radial distribution function and for the potential of mean force for octa-functionalized POSS monomers dissolved in PDMS at 300, 400, 600, and 1000 K. Contrary to the results obtained for bare POSS monomers, the results shown in Figure 6 manifest a remarkable dependence on temperature. At 300 K, the radial distribution function presents an intense attractive peak at a center-to-center separation of approximately 0.88 nm followed by weak midrange repulsion and by a substantial long-range attractive peak. As the temperature increases, the short-range attraction becomes less intense, the attractive peak shifts at larger center-to-center separations (0.92 nm at 400 K, 0.94 nm at 600 K, and 0.96 nm at 1000 K), the midrange repulsion becomes more significant, the long-range attraction becomes weaker, and the profile of the pair correlation function becomes smoother. Results obtained at 600 and 1000 K are similar to each other, the only appreciable

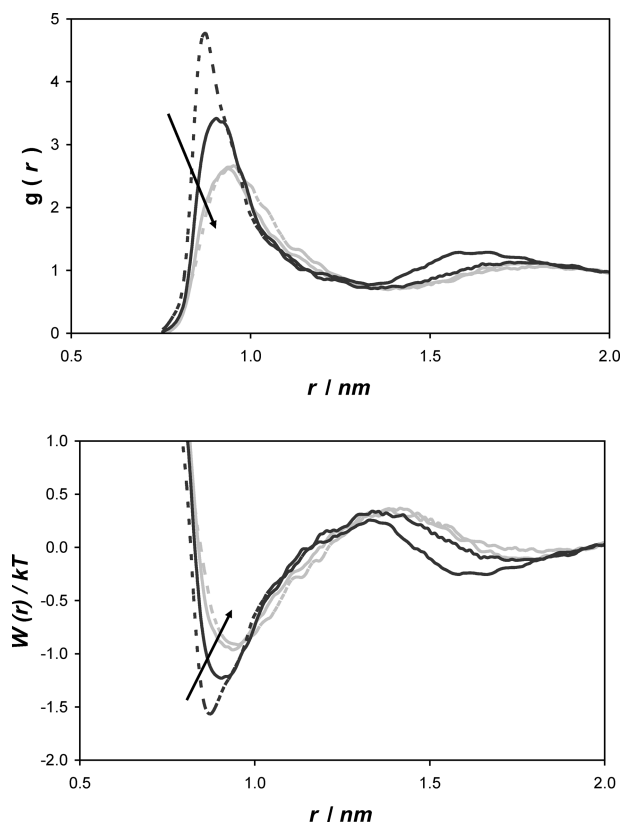


Figure 6. Radial distribution function (top) and effective pair potential of mean force (bottom) between octa-functionalized POSS monomers dissolved in PDMS as a function of the center-to-center distance between centers of mass of the POSS monomers. Results are reported for several temperatures: black dotted lines for 300 K, black solid lines for 400 K, gray solid lines for 600 K, and gray dotted lines for 1000 K. Statistical uncertainties are not reported for clarity. The arrows indicate results obtained as the temperature increases.

difference being the width of the attractive peak at short separation, which becomes slightly wider at higher temperatures reflecting higher molecular mobility.

To address the issue of the effect of system size on the calculated properties, we simulate a system composed of 10 octa-functionalized POSS monomers in solution with 81 PDMS chains. The simulation procedure is the same as that described earlier, but the box size is 6.0 nm. In Figure 7, we compare the effective pair potential of mean force between the POSS monomers when the box size is either 4.0 or 6.0 nm. While the results do not coincide perfectly, we note that the difference between the data sets is within the statistical uncertainty of our calculations.

Diffusion Coefficient. In Figure 8, we report the mean-square displacement (ΔR^2) of octa-functionalized POSS cubes in PDMS at different temperatures. The mean-square displacement indicates that POSS monomers dissolved in PDMS are subject to motion according to Fickian diffusion. Some anomalous diffusion is observed only at short times. To evaluate the diffusion coefficient, we fit the Einstein expression (eq 7) to the simulated mean-square displacement at long times.

As discussed by Müller-Plathe et al.,⁵⁵ when small molecules are dissolved in polymeric systems their diffusion pathways may be altered due to the surrounding structure that induces additional tortuosity, as if a molecule was moving in a labyrinth. This type of additional constraint is reflected in a motion characterized by a “hopping” pattern. In a hopping pattern, a solute molecule oscillates for long periods of time in defined positions, usually the voids in the amorphous polymer matrix,

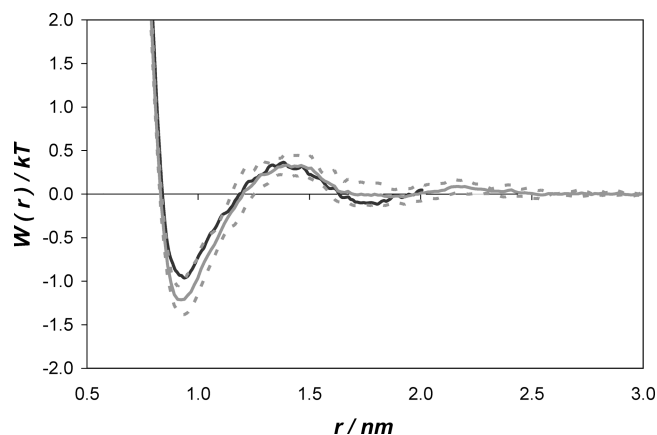


Figure 7. Effective pair potential of mean force between octa-functionalized POSS monomers dissolved in PDMS as a function of the center-to-center distance between the centers of mass of the POSS monomers. Results are reported for different simulation box sizes. The black line is for a 4.0 nm box size, and the gray solid line is for a 6.0 nm box size. The gray dotted lines delimit the statistical uncertainty for the results obtained in the 6.0 nm simulation box.

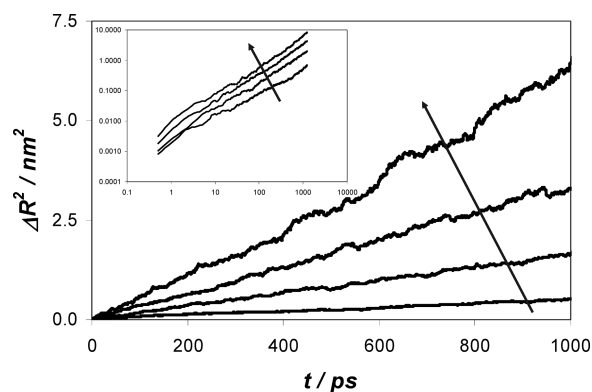


Figure 8. Mean-square displacement as a function of time for octa-functionalized POSS monomers in PDMS. Results were obtained at 300, 400, 600, and 1000 K. The arrow indicates results obtained as the temperature increases. In the inset, we report the double logarithmic plot for the mean-square displacement.

and occasionally moves very fast to reach a neighboring void.^{56,57} To characterize the motion of POSS monomers diluted in PDMS, we report in Figure 9 the displacement of selected octa-functionalized POSS monomers as a function of time.

The results shown in Figure 9 show several points (circled) at which the motion of silsesquioxane monomers is characterized by fast jumps from one position to another (several tenths of a nanometer away) followed by periods during which the center of mass of the POSS monomers oscillates around a fixed position (this mechanism is particularly evident for results obtained at 400 and 600 K). In the trajectory of octa-functionalized POSS monomers in PDMS at 300 K, the displacement from the initial position increases gradually as time increases. Several short hops can be observed in the results shown in Figure 9, but they correspond to rare events, probably because at this temperature the motion of simulated PDMS chains is slow. As a consequence, longer simulation runs may be required to estimate the self-diffusion coefficient of dissolved POSS monomers at 300 K. This limitation affects the reliability of the self-diffusion coefficients estimated for POSS monomers dissolved in PDMS at 300 K. At 1000 K, our results indicate that POSS monomers possess greater mobility and often hop between different close locations within the polymer melt. These qualitative observations are corroborated by visualization of sequences of simulation snapshots. The animations suggest that

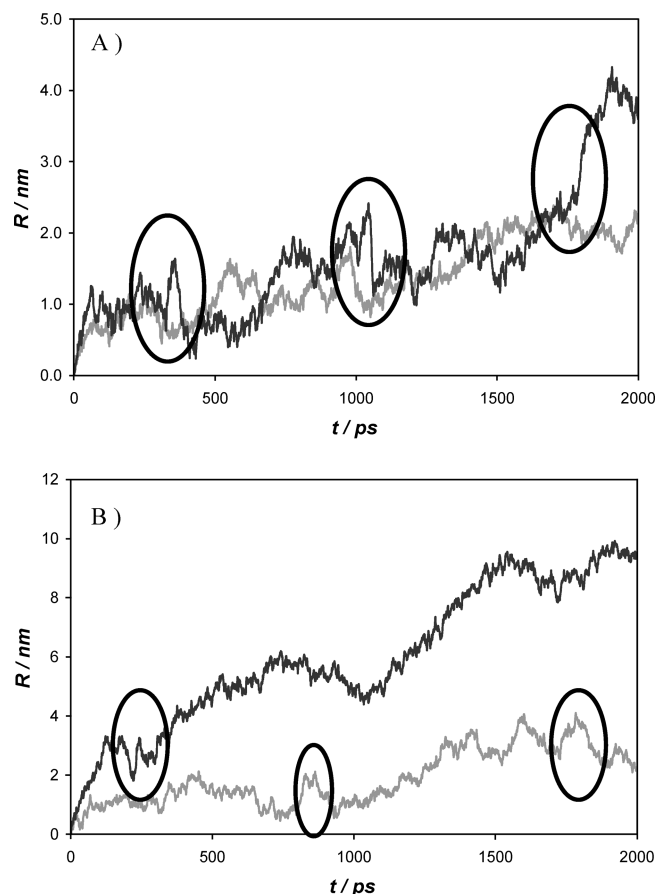


Figure 9. Displacement R as a function of time for selected octa-functionalized POSS monomers in PDMS. Panel A is for results obtained at 300 (gray line) and 400 K (black line); panel B is for results obtained at 600 (gray line) and 1000 K (black line). The circles highlight rare hopping events, discussed in the text.

when POSS monomers approach each other they promote density fluctuations in the surrounding polymeric system, thus provoking the hops of the POSS monomers from one position to another.

When the diffusion of a molecule in a polymeric system is described as an activated process such as the hopping mechanism, the diffusion coefficient should depend on temperature according to an Arrhenius-type mathematical function:⁵⁸

$$D = D_0 \exp(-E_A/kT) \quad (8)$$

where D_0 is a constant and E_A is the activation energy. In Figure 10, we report both the simulated self-diffusion coefficient as a function of temperature and the Arrhenius plot for bare and octa-functionalized POSS monomers in PDMS. Our results indicate that at >400 K eq 8 is obeyed. However, the diffusion coefficient estimated from simulation results at 300 K does not follow the Arrhenius dependence. This discrepancy is probably due to the fact that our simulation runs are too short to evaluate the diffusion coefficients for POSS monomers in PDMS at 300 K, as mentioned earlier. Thus, we suspect that the extrapolation of eq 8 at 300 K yields a more reliable estimate for the diffusion coefficient at that temperature than the direct simulations. For comparison purposes, we also compute the diffusion coefficients of the centers of mass of the PDMS chains considered in our simulations. We display the results in Figure 10. As a test of our results, we compared the diffusion coefficients obtained from our simulations with those obtained for isoprene polymers with 40–115 monomers.⁵⁹ The diffusion coefficients obtained for

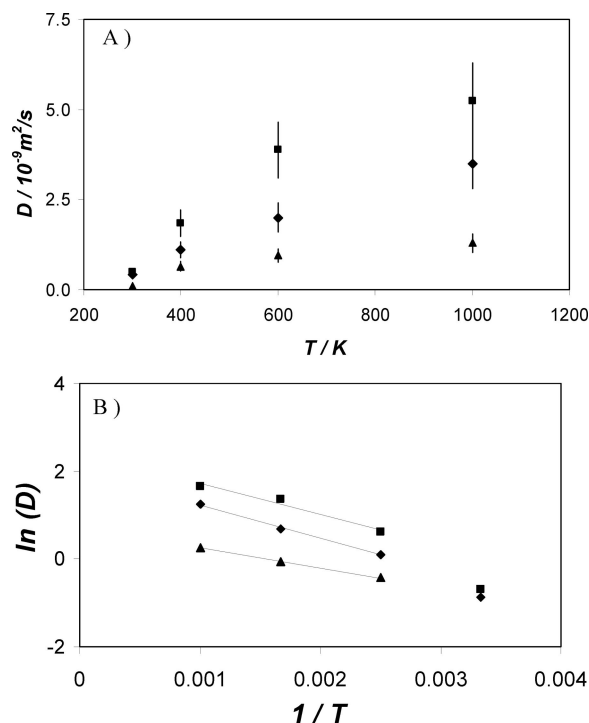


Figure 10. Self-diffusion coefficient as a function of temperature (A) and Arrhenius plot for the self-diffusion coefficient (B). Results are for the center of mass of the PDMS molecules (gray triangles), dissolved bare POSS monomers (black squares), and octa-functionalized POSS monomers (black diamonds). The lines are the best linear fit obtained here. Self-diffusion coefficients computed at 300 K were not used for the data regression.

the PDMS chains are 1 order of magnitude larger than those for the isoprene chains, which seems to be physically reasonable since the diffusion coefficient decreases as the molecular weight of a molecule increases.

Summary

In this work, we have used canonical (NVT) molecular dynamics algorithms to compute the thermodynamic and transport properties of polyhedral oligomeric silsesquioxane monomers dissolved in poly(dimethylsiloxane) at 300, 400, 600, and 1000 K. The POSS monomers considered are either bare (hydrogen-terminated) or octa-functionalized. In the octa-functionalized POSS monomers, the hydrogen atoms of the bare POSS monomers are substituted with methyl groups. We have reported here the first simulated data for the POSS–POSS center-to-center radial distribution function and potential of mean force and for the self-diffusion coefficients for silsesquioxanes dissolved in polymeric systems. Our simulations show that silsesquioxanes dissolved in PDMS attract each other under all the conditions that have been considered. In addition, our calculations demonstrate that it is possible to tailor the effective POSS–POSS interactions by changing the system temperature and/or by substituting the hydrogen atoms in the bare silsesquioxane monomers with appropriate functional groups. Our simulations also show that the diffusion of POSS monomers dissolved in PDMS occurs by a hopping mechanism, typical of small molecules dissolved in polymeric systems. The self-diffusion coefficient depends on temperature according to the Arrhenius relationship at temperatures in the range of 400–1000 K.

Acknowledgment. We acknowledge financial support from the U.S. National Science Foundation under Contract DMR-

0103399. Calculations were performed on the VAMPIRE cluster at Vanderbilt University (Nashville, TN) and at the NERSC facilities (Berkeley, CA). A.S. thanks P. K. Naicker and A. Jayaraman for interesting discussions and encouragement.

References and Notes

- (1) Giannelis, E. P. *Adv. Mater.* **1996**, *8*, 29.
- (2) LeBaron, P. C.; Wang, Z.; Pinnavaia, T. J. *J. Appl. Clay Sci.* **1999**, *15*, 11.
- (3) Tsagaropoulos, G.; Eisenberg, A. *Macromolecules* **1995**, *28*, 6067.
- (4) Paxton, J. P.; Mowles, E. D.; Eric, D.; Lukehart, C. M.; Witzig, A. *J. Proceedings of the American Society for Composites, 16th Technical Conference*; 2001; p 565.
- (5) Hawker, C. J.; Fréchet, J. M. J. *J. Am. Chem. Soc.* **1990**, *112*, 7638.
- (6) Gauthier, M.; Möller, M. *Macromolecules* **1991**, *24*, 4548.
- (7) Striolo, A.; Prausnitz, J. M.; Bertuccio, A.; Kee, R. A.; Gauthier, M. *Polymer* **2001**, *42*, 2579.
- (8) POSS is a trademark of Hybrid Plastics (www.hybridplastics.com).
- (9) Shockey, E. G.; Bolf, A. G.; Jones, P. F.; Schwab, J. J.; Chaffee, K. P.; Haddad, T. S.; Lichtenhan, J. D. *Appl. Organomet. Chem.* **1999**, *13*, 311.
- (10) Lichtenhan, J. D. *Commun. Inorg. Chem.* **1995**, *17*, 115.
- (11) Shockey, E. G.; Bolf, A. G.; Jones, P. F.; Schwab, J. J.; Chaffee, K. P.; Haddad, T. S.; Lichtenhan, J. D. *Appl. Org. Chem.* **1999**, *13*, 311.
- (12) Feher, F. J.; Newman, D. A.; Walzer, J. F. *J. Am. Chem. Soc.* **1989**, *111*, 1741.
- (13) Jeoung, E.; Carroll, J. B.; Rotello, V. M. *Chem. Commun.* **2002**, 1510.
- (14) Cassagneau, T.; Caruso, F. *J. Am. Chem. Soc.* **2002**, *124*, 8172.
- (15) Bellas, V.; Tegou, E.; Raptis, I.; Gogolides, E.; Argitis, P.; Iatron, H.; Hadjichristidis, N.; Sarantopoulou, E.; Cefalas, A. C. *J. Vac. Sci. Technol.* **2002**, *B20*, 2902.
- (16) Feher, F. J.; Weller, K. J. *Inorg. Chem.* **1991**, *30*, 880.
- (17) Duchateau, R.; Abbenhuis, H. C. L.; van Santen, R. A.; Meetsma, A.; Thiele, S. K.-H.; van Tol, M. F. H. *Organometallics* **1998**, *17*, 5663.
- (18) Maka, K.; Itoh, H.; Chujo, Y. *Nano Lett.* **2002**, *2*, 1183.
- (19) Carroll, J. B.; Frankamp, B. L.; Srivastava, S.; Rotello, V. M. *J. Mater. Chem.* **2004**, *14*, 690.
- (20) Kim, K.-M.; Keum, D.-K.; Chujo, Y. *Macromolecules* **2003**, *36*, 867.
- (21) Kim, B.-S.; Mather, P. T. *Macromolecules* **2002**, *35*, 8378.
- (22) Deng, J.; Hottle, J. R.; Polidan, J. T.; Kim, H.-J.; Farmer-Creely, C. E.; Viers, B. D.; Esker, A. R. *Langmuir* **2004**, *20*, 109.
- (23) Len, C.-M.; Reddy, G. M.; Wei, K.-H.; Shu, C.-F. *Chem. Mater.* **2003**, *15*, 2261.
- (24) Len, C.-M.; Chang, Y.-T.; Wei, K.-H. *Macromolecules* **2003**, *36*, 9122.
- (25) Ropartz, L.; Foster, D. F.; Morris, R. E.; Slawin, A. M. Z.; Cole-Hamilton, D. J. *J. Chem. Soc., Dalton Trans.* **2002**, *9*, 1997.
- (26) Mengel, C.; Meyer, W. H.; Wegner, G. *Macromol. Chem. Phys.* **2001**, *202*, 1138.
- (27) Neumann, D.; Fisher, M.; Trau, L.; Matisons, J. G. *J. Am. Chem. Soc.* **2002**, *124*, 13998.
- (28) Fu, B. X.; Yang, L.; Somani, R. H.; Zong, S. X.; Hsiao, B. S.; Phillips, S.; Blanski, R.; Ruth, P. J. *J. Polym. Sci., Part B: Polym. Phys.* **2001**, *39*, 2727.
- (29) Lee, A.; Lichtenhan, J. D. *J. Appl. Polym. Sci.* **1999**, *73*, 1993.
- (30) Lichtenhan, J. D.; Vu, N. Q.; Carter, J. A.; Gilman, J. W.; Feher, F. J. *Macromolecules* **1993**, *26*, 2141.
- (31) Lichtenhan, J. D.; Otonari, Y. A.; Carr, M. J. *Macromolecules* **1995**, *28*, 8435.
- (32) Pyun, J.; Matyjaszewski, K.; Wu, J.; Kim, G.-M.; Chun, S. B.; Mather, P. T. *Polymer* **2003**, *44*, 2739.
- (33) Romo-Uribe, A.; Mather, P. T.; Haddad, T. S.; Lichtenhan, J. D. *J. Polym. Sci., Part B: Polym. Phys.* **1998**, *36*, 1857.
- (34) Jeon, H. G.; Mather, P. T.; Haddad, T. S. *Polym. Int.* **2000**, *49*, 453.
- (35) Fu, B. X.; Hsiao, B. S.; Pagoda, S.; Stephens, P.; White, H.; Rafailovich, M.; Sokolov, J.; Mather, P. T.; Jeon, H. G.; Phillips, S.; Lichtenhan, J.; Schwab, J. *Polymer* **2001**, *42*, 599.
- (36) Xu, H.; Kuo, J.-W.; Lee, J.-S.; Chang, F.-C. *Macromolecules* **2002**, *35*, 8788.
- (37) Zheng, L.; Waddon, A. J.; Farris, R. J.; Coughlin, E. B. *Macromolecules* **2002**, *35*, 2375.
- (38) Zheng, L.; Farris, R. J.; Coughlin, E. B. *Macromolecules* **2001**, *34*, 8034.
- (39) Schwab, J. J.; Haddad, T. S.; Lichtenhan, J. D.; Mather, P. T.; Chaffee, K. P. *Antec* **1997**, *611*, 1817.
- (40) Phillips, S. H.; Haddad, T. S.; Tomczak, S. J. *Curr. Opin. Solid Stat Mater. Sci.* **2004**, *8*, 21.
- (41) Waddon, A. J.; Zheng, L.; Farris, R. J.; Coughlin, E. B. *Nano Lett.* **2002**, *2*, 1149.
- (42) Choi, J.; Yee, A. F.; Laine, R. M. *Macromolecules* **2003**, *36*, 5666.
- (43) Bharadwaj, R. K.; Berry, R. J.; Farmer, B. L. *Polymer* **2000**, *41*, 7209.
- (44) Lamm, M. H.; Chen, T.; Glotzer, S. C. *Nano Lett.* **2003**, *3*, 989.
- (45) Müller-Plathe, F. *Chem. Phys. Chem.* **2002**, *3*, 754.
- (46) Striolo, A.; Tavares, F. W.; Bratko, D.; Blanch, H. W.; Prausnitz, J. M. *J. Phys. Chem. Chem. Phys.* **2003**, *5*, 4851.
- (47) Frischknecht, A. L.; Curro, J. G. *Macromolecules* **2003**, *36*, 2122.
- (48) Martin, M. G.; Siepmann, J. I. *J. Phys. Chem. B* **1998**, *102*, 2569.
- (49) Smith, W.; Forester, T. J. *Mol. Graphics* **1996**, *14*, 136.
- (50) Allen, M. P.; Tildesley, D. J. *Computer Simulation of Liquids*; Oxford University Press: New York, 1987.
- (51) Striolo, A.; Colina, C. M.; Elvassore, N.; Gubbins, K. E.; Lue, L. *Mol. Sim.* **2004**, *30*, 437.
- (52) Chandler, D. *Introduction to Modern Statistical Mechanics*; Oxford University Press: New York, 1987.
- (53) Tavares, F. W.; Bratko, D.; Striolo, A.; Blanch, H. W.; Prausnitz, J. M. *J. Chem. Phys.* **2004**, *120*, 9859.
- (54) Patel, N.; Egorov, S. A. *J. Chem. Phys.* **2004**, submitted for publication.
- (55) Müller-Plathe, F.; Rogers, S. C.; van Gunsteren, W. F. *Chem. Phys. Lett.* **1992**, *199*, 237.
- (56) Müller-Plathe, F. *J. Chem. Phys.* **1991**, *94*, 3192.
- (57) Hahn, O.; Mooney, D. A.; Müller-Plate, F.; Kremer, K. *J. Chem. Phys.* **1999**, *111*, 6061.
- (58) Pauli, S. In *Polymer Handbook*, 3rd ed.; Brandrup, J., Immergut, E. H., Eds.; Wiley: New York, 1989.
- (59) Doxastakis, M.; Theodorou, D. N.; Fytas, G.; Kremer, F.; Fallor, R.; Müller-Plate, F.; Hadjichristidis, N. *J. Chem. Phys.* **2003**, *119*, 6883.